Available online at www.sciencedirect.com

ScienceDirect

Procedia Structural Integrity 5 (2017) 255–262

Structural Integrity Procedia

www.elsevier.com/locate/procedia

2nd International Conference on Structural Integrity, ICSI 2017, 4-7 September 2017, Funchal, Madeira, Portugal

Weak and strong bi-material interfaces and their influence on propagating cracks in plane elastic structures

Johannes Scheel[a,]*, Andreas Ricoeur[a]

[a]*University of Kassel, Institute of Mechanics, Mönchebergstraße 7, D-34125 Kassel, Germany*

Abstract

The developing crack paths in heterogeneous structures are the result of the inhomogeneous state of stress. The latter stems from e.g. voids or inclusions in an elastic matrix, which are bonded either by strong or weak interfaces. Besides the stiffness of an inclusion, the kind of interface has a decisive influence on the state of stress and therefore on propagating cracks. It is experimentally proven that cracks tend to grow towards regions with lower stiffness (Tilbrook et al., 2006; Judt et al., 2015), therefore matrix cracks might be attracted by interface delamination cracks. In this research the matrix crack growth in bi-material structures is simulated, incorporating dissipative processes arising at weak interfaces and a reference is provided by simulating the crack propagation in the same bi-material but with a strong (perfect) interface. Incremental crack extensions constitute the matrix crack growth, requiring a continuous modification of the geometry. An intelligent re-meshing procedure is applied, where the loading history cannot be neglected due to the presence of dissipative processes (Judt and Ricoeur, 2013b). The crack deflection and crack tip loading are determined by the J-integral criterion and the energy release rate, respectively. The resulting crack paths confirm that the matrix crack tends to grow into the direction of regions with lower stiffness. If weak interfaces are considered, an extremely attracting effect on propagating matrix cracks caused by the delamination is observed, which is stronger than the influence of divergent stiffnesses.

Peer-review under responsibility of the Scientific Committee of ICSI 2017

Keywords: Crack growth simulation; interface debonding; cohesive zones; J-integral criterion; delamination

* Corresponding author. Tel.: +49-561-804-2824.
E-mail address: j.scheel@uni-kassel.de

2452-3216
Peer-review under responsibility of the Scientific Committee of ICSI 2017
10.1016/j.prostr.2017.07.127

1. Introduction

Predicting crack paths in engineering structures is a complex procedure due to the many influencing effects that can arise. In the case of heterogeneous materials, e.g. polymers or adhesives with incorporated fibers or microcapsules, crack tip loading and crack deflection depend on the emerging stress state due to these inclusions. In this work an elastic matrix and an inclusion are considered, which are connected by bi-material interfaces. These interfaces are either assumed to be strong (perfect) or weak (imperfect). The imperfect interfaces are modelled with cohesive zones, so that delamination cracks can develop. One goal is to investigate the interaction of a matrix crack with strong and weak bi-material interfaces and its influence on propagation paths. In order to determine crack growth thresholds and deflection angles it is necessary to quantify the crack tip loading. Therefore the objective is not only to simulate the matrix and interface crack propagation in bi-material structures, but also to investigate influences of inclusion and interface parameters on the crack tip loading quantities. The J-integral criterion is an appropriate means to predict crack deflection, assuming the crack will extend incrementally in the direction of the J-integral vector, thus leading to a maximum reduction of total potential energy.

Nomenclature

a_0	initial crack length
D_{ij}	damage tensor/matrix
$d_{n/s}$	scalar damage variable (normal/shear)
E	Young's modulus
F^{cz}	specific Helmholtz free energy of the cohesive zone
G	energy release rate
$G^c_{I/II}$	critical energy release rate (mode I / II)
J_k	J-integral vector
K_{Ic}	fracture toughness
K_{jk}	stiffness tensor/matrix
n_j	normal vector on an integration contour
Q_{kj}	energy momentum tensor
r	radius
t_i	traction vector
$t^c_{n/s}$	critical traction
u_i	displacement vector
z_k	crack growth direction unit vector
Γ	integration contour
δ_i	separation (displacement jump) vector
δ_{ij}	Kronecker delta/ identity tensor
$\delta^0_{n/s}$	damage onset separation
$\delta^c_{n/s}$	critical separation
$\delta^{max}_{n/s}$	maximum attained separation
ò	integration contour radius
ν	Poisson's ratio

2. Fracture mechanical approaches

In order to simulate the matrix crack propagation, the bi-material interfaces need to be introduced. In perfect interfaces the displacement u_i and the traction vector t_i are continuous. Consequently, no delamination or damage, respectively, results from loading (Hashin, 2002). At weak cohesive interfaces, on the other hand, there is no continuity of displacements and not necessarily of tractions. The behaviors of the associated surfaces of the interface

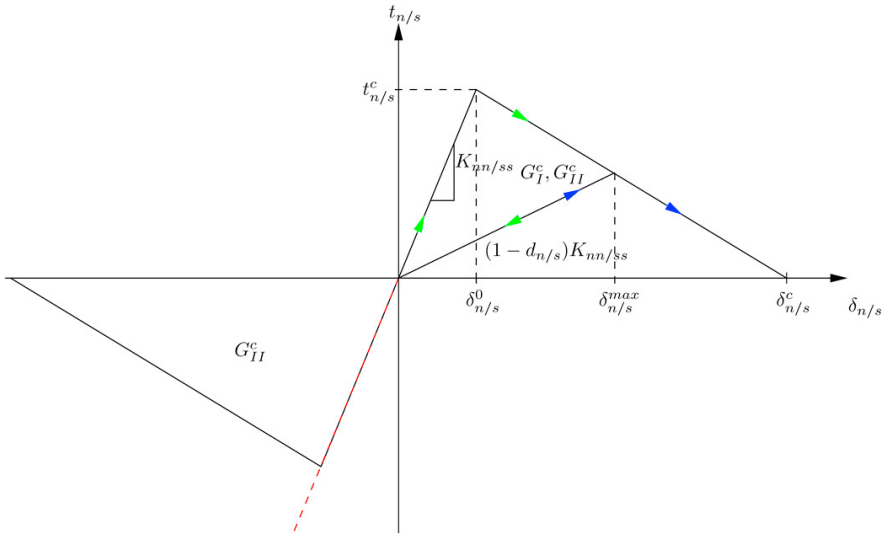

Fig. 1 Bilinear cohesive law for normal and shear (mode I/II) separation

are represented by cohesive laws, relating the cohesive tractions and the displacement jump/separation δ_i . Disregarding heat flux or temperature changes, furthermore introducing some spatial simplifications in the energy balance (Ottosen et al., 2015) and assuming infinitesimal deformation, the dissipation or Clausius Duhem inequality for this specific case reads

$$\begin{aligned} 0 &\leq -\dot{F}^{CZ}(\delta_i, D_{ij}) + \dot{\delta}_i t_i \\ 0 &\leq \left[t_i - \frac{\partial F^{CZ}(\delta_i, D_{ij})}{\partial \delta_i}\right]\dot{\delta}_i - \frac{\partial F^{CZ}(\delta_i, D_{ij})}{\partial D_{ij}}\dot{D}_{ij} \quad , \end{aligned} \tag{1}$$

where F^{CZ} is the specific Helmholtz free energy of the cohesive zone associated with any reference surface between the positive and negative surfaces of the cohesive zone and t_i is the traction vector associated with the same surface. The analytical notation is used for tensor operations, implying summation over repeated indices holding values 1 and 2. Neglecting coupling of the damage evolution in normal and shear directions in a plane problem, the Helmholtz free energy of a bilinear cohesive law is introduced as

$$F^{CZ} = \frac{1}{2}\delta_i(\delta_{ij} - D_{ij})K_{jk}\delta_k \quad , \tag{2}$$

where δ_{ij} is the Kronecker delta, K_{jk} the stiffness tensor and D_{ij} the damage tensor, i.e. the matrix in which the scalar damage variables for the two loading modes are stored:

$$K_{jk} = \begin{bmatrix} K_{nn} & 0 \\ 0 & K_{ss} \end{bmatrix}; \quad D_{ij} = \begin{bmatrix} A & 0 \\ 0 & B \end{bmatrix} \quad \text{with} \quad A = \begin{cases} d_n & \forall d_s < 1 \\ 1 & , d_s = 1 \end{cases} \quad \text{and} \quad B = \begin{cases} d_s & \forall d_n < 1 \\ 1 & , d_n = 1 \end{cases} \quad . \tag{3}$$

The classical fracture mechanical crack opening modes are used to distinguish between a normal (mode *I*, normal to the crack faces) and a shear (mode *II*, tangential to the crack faces) loading of the interface crack. The partial derivative of the Helmholtz free energy with respect to the separation results in the bilinear cohesive law depicted in Fig. 1

$$t_i = \frac{\partial F^{CZ}(\delta_i, D_{ij})}{\partial \delta_i} = (\delta_{ij} - D_{ij})K_{jk}\delta_k \quad , \tag{4}$$

with the areas under the curves describing the critical energy release rates G_I^c or G_{II}^c for the two loading modes. For positive normal separation the same parameters are assumed as for shear loading, but for a negative separation, softening will not occur for normal loading, avoiding penetration and damage. Inserting Eq. (4) into the dissipation inequality (1) yields

$$-\frac{\partial F^{CZ}(\delta_i, D_{ij})}{\partial D_{ij}} \dot{D}_{ij} \geq 0 \quad , \tag{5}$$

where the irreversibility of the damage evolution, i.e. $\dot{D}_{ij} \geq 0$, leads to the condition

$$\frac{\partial F^{CZ}(\delta_i, D_{ij})}{\partial D_{ij}} \leq 0 \quad . \tag{6}$$

With the Helmholtz free energy according to Eq. (2) the derivative reads

$$\frac{\partial F^{CZ}(\delta_i, D_{ij})}{\partial D_{ij}} = -\frac{1}{2} \delta_i K_{jk} \delta_k \quad , \tag{7}$$

so that the requirement for thermodynamic consistency of Eq. (6) is fulfilled, as long as the stiffness matrix K_{jk} is positive definite. In Fig. 1 the maximum value of the separation for each loading mode attained during the loading history is denoted as $\delta_{n/s}^{max}$, so that the scalar damage variables d_n, d_s can be calculated by

$$d_{n/s} = \frac{\delta_{n/s}^c (\delta_{n/s}^{max} - \delta_{n/s}^0)}{\delta_{n/s}^{max} (\delta_{n/s}^c - \delta_{n/s}^0)} \quad , \tag{8}$$

where $d_{n/s} \in [0,1]$. With the assumptions made, three independent parameters, e.g. $K_{nn/ss} = K$, $\delta_{n/s}^0 = \delta^0$, $G_{I/II}^c = G^c$ need to be set in order to define the cohesive law, the other parameters are calculated as

$$t^c = K\delta^0 \quad ; \quad \delta^c = \frac{2G^c}{t^c} \quad . \tag{8}$$

The matrix crack growth is simulated by incremental crack extensions, leading to a continuous modification of the geometry. Intelligent re-meshing is therefore required (Judt and Ricoeur, 2013a; Judt et al., 2015). The loading history cannot be neglected due to the dissipative processes in the cohesive zone. It is taken into account by the damage variables $d_{n/s}$ which are stored and passed on during the calculations. The J-integral is calculated to determine the matrix crack tip loading and the matrix crack deflection is calculated applying the J-integral criterion. Remote integration contours like Γ in Fig. 2 are applied, providing the correct crack tip loading quantity in terms of path independence, if curved cracks, bi-material interfaces or holes are accounted in the formulation of the J-integral:

$$\begin{aligned} J_k &= \lim_{\dot{o} \to 0} \int_{\Gamma_{\dot{o}}} Q_{kj} n_j ds \\ &= \lim_{\dot{o} \to 0} \int_{\Gamma^+ + \Gamma^-} Q_{kj} n_j ds + \int_{\Gamma_0} Q_{kj} n_j ds + \int_{\Gamma_A} Q_{kj}^A n_j^A ds + \int_{\Gamma_B} Q_{kj}^B n_j^B ds \end{aligned} \quad . \tag{10}$$

Volumetric forces are neglected and Q_{kj} is the energy momentum tensor. The crack face integrals Γ^+ / Γ^- require special treatment to improve their accuracy (Judt and Ricoeur, 2013a). The integral along Γ_B always vanishes, no matter if a hole or an inclusion is modelled, since the surrounded domain is free from defects. The energy release rate equals the projection of the J-integral vector on the unit crack growth direction vector z_k

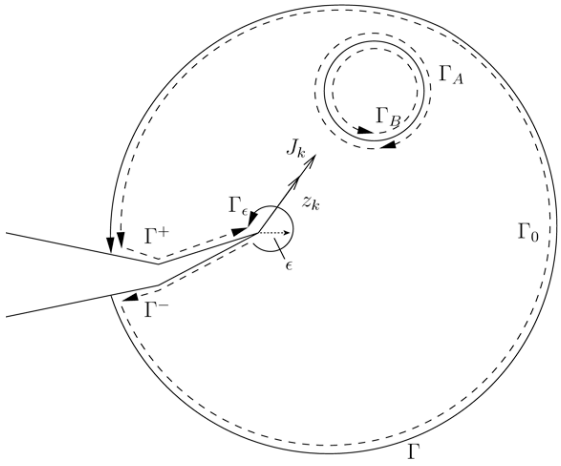

Fig. 2 Integration contours for the J-integral

$$G = J_k z_k \quad , \tag{11}$$

so that the crack grows into the direction of the J-integral vector as the energy release rate reaches its maximum (Judt et al., 2015) .

3. Results of the crack growth simulation

In this work plane elastic structures are considered with circular inclusions as illustrated in Fig. 3. Both models are identical, except for the position of the inclusion. They both have an initial crack length of $a_0 = 10\,\text{mm}$ and the inclusion radius is $r = 7\,\text{mm}$. A monotonically increasing displacement load u is applied so that the matrix crack growth simulation represents critical fracture conditions. The material of the inclusion is varied for different simulations according to

$$\begin{aligned}
&\text{Material A} \qquad E = 3039 \;\; \text{MPa}; \;\; \nu = 0.37; \;\; K_{Ic} = 32 \;\; \text{MPa}\sqrt{\text{mm}},\\
&\text{Material B} \qquad E = 1230 \;\; \text{MPa}; \;\; \nu = 0.37,\\
&\text{Material C} \qquad E = 7509 \;\; \text{MPa}; \;\; \nu = 0.37,
\end{aligned}$$

where E is Young's modulus, ν Poission's ratio and K_{Ic} the fracture toughness. Material A represents experimental data of an epoxy resin and materials B and C are hypothetical softer or stiffer materials. The fracture toughness of material A has not yet been determined, hence it was assumed in the range of other epoxy resins. The parameters of the imperfect interface between inclusion and matrix are chosen as:

$$\begin{aligned}
K = \;\; & 7000\,\frac{\text{N}}{\text{mm}^3}; \;\; \delta^0 = 0.0005\,\text{mm}; \;\; G^c = 0.0525\,\frac{\text{N}}{\text{mm}}\\
\Rightarrow \;\; & t^c = 3.5\,\text{MPa}; \;\; \delta^c = 0.03\,\text{mm}
\end{aligned} \quad . \tag{12}$$

Besides inclusions, a circular void or hole is implemented as a limiting case.

The resulting crack paths are shown in Figure 4. The crack is growing in the elastic matrix consisting of material A and the inclusion is modelled as either a softer core (material B), a stiffer core (material C) or as a hole. If a strong interface is considered, the matrix crack is slightly deflected either in the direction of the inclusion for a softer core

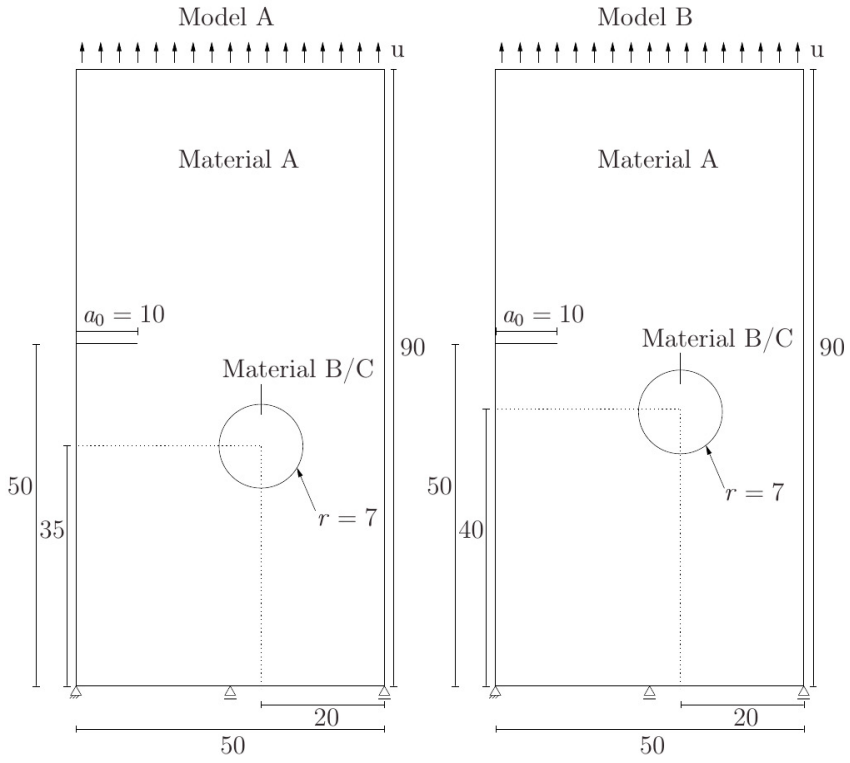

Fig. 3 Models for the crack growth simulation (size in mm)

or away from it for a stiffer core. If a hole is considered, the deflecting effect is even more intense. These results illustrate, that the matrix cracks tend grow into the direction of lower Young's modulus and away from regions with a higher stiffness, which is in good agreement with the results of Judt et al. (2015), Kikuchi et al. (2016) and Tilbrook et al. (2006). The deflection going along with the weak interfaces, however, is by far more pronounced. The matrix crack in connection with a weak interface and a stiff core is even more attracted by the inclusion than the crack in connection with a soft core and a strong or weak interface. That might be in contradiction to the results with a strong interface but because of the stiffer inclusion, less deformation occurs and thus the interface is more stressed, leading to an augmented softening and interface damage. A weakened interface is even more attractive for the matrix crack than a hole. In the case of the closer positioned inclusion (Fig. 4 b)), a weak interface is always more attractive for matrix cracks than a hole, no matter if the inclusion is softer or stiffer. The figure also shows the effect of the distance of the incipient crack with respect to the interface. The smaller it is, the larger are the observed deflections, so that cracks tend to intersect the inclusion or hole in Fig. 4 b) whereas cracks in Fig. 4 a) grow past it.

4. Crack tip loading

In order to determine the effect of softening at a weak interface on the matrix crack tip loading, the model of Fig. 5 a) is investigated. The inclusion shares the same material as the elastic matrix. The interface is either modelled perfect or imperfect and a hole is implemented for comparison. For the imperfect interfaces the stiffness, critical energy release rate and traction are varied to investigate the emerging effect, see Table 1. In Fig. 5 b) the crack tip loading is depicted by means of the energy release rate plotted versus the normalized displacement loading. The energy release rates for the weak interfaces are similar to the energy release rate calculated with a perfect interface until damage occurs. One could suppose that the crack tip loading is always reduced due to the dissipated energy at

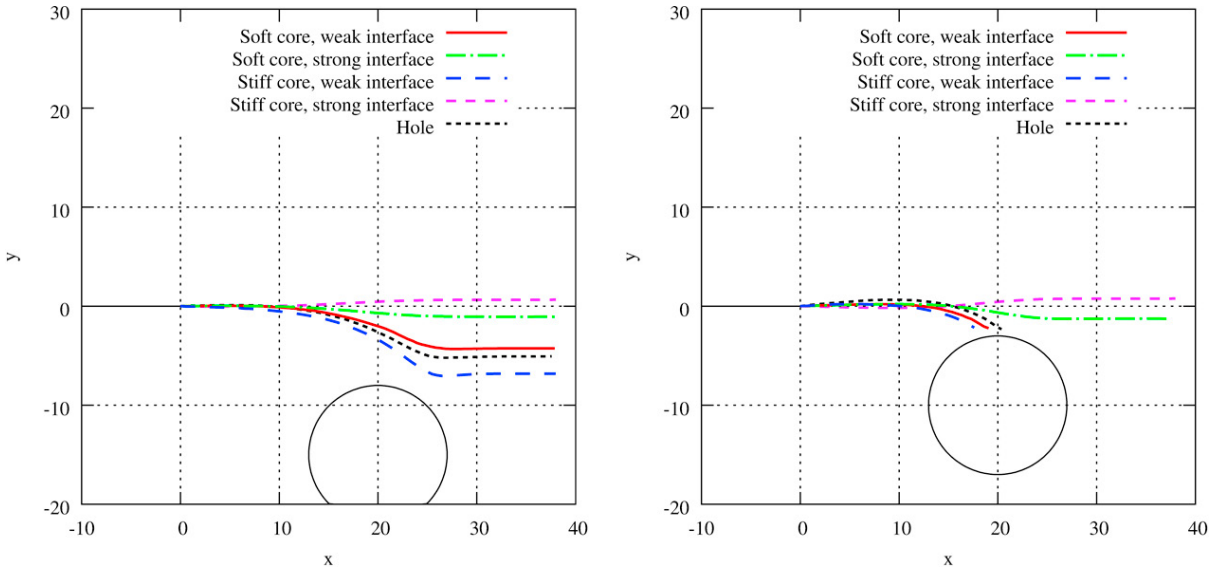

Fig. 4 Crack paths of the simulation for a) model A, b) model B. Soft core = material B, stiff core = material C

the interface when damage develops, but this is obviously not the case, being in agreement with the results of Judt and Ricoeur (2016). It is obvious that a softer and thus a more damaged interface results in a larger crack tip loading, approaching and finally even slighlty exceeding the crack tip loading in connection with a hole. In this study, the energy release rate of the matrix crack in connection with an arbitrary weak interface is always larger than for the perfect interface. This is not obligatory, however, depending on the alignment and shape of crack and interface.

Table 1. Cohesive law parameters for the crack tip loading investigation

Cohesive parameters	K [N/mm^3]	δ^0 [mm]	G^c [N/mm]	t^c [MPa]	δ^c [mm]
a)	10000	0.0005	0.075	5	0.03
b)	7000	0.0005	0.0525	3.5	0.03
c)	4000	0.0005	0.03	2	0.03

5. Conclusions

Crack paths were simulated for matrix cracks in bi-material structures with internal circular strong and weak interfaces. The matrix cracks tend to grow into the direction of lower stiffness and are repelled by stiff domains. The deflection caused by a weak interface and the related delamination, however, is by far more pronounced, attracting a matrix crack even if a stiff inclusion is implemented. The distance to the interface has a considerable influence on the deflection. The stiffnesses of the imperfect interfaces also have a significant influence on the crack tip loading. In this case, a softer interface always increases it compared to the crack tip loading near a perfect interface, even exceeding values of calculations with a hole for very weak interfaces.

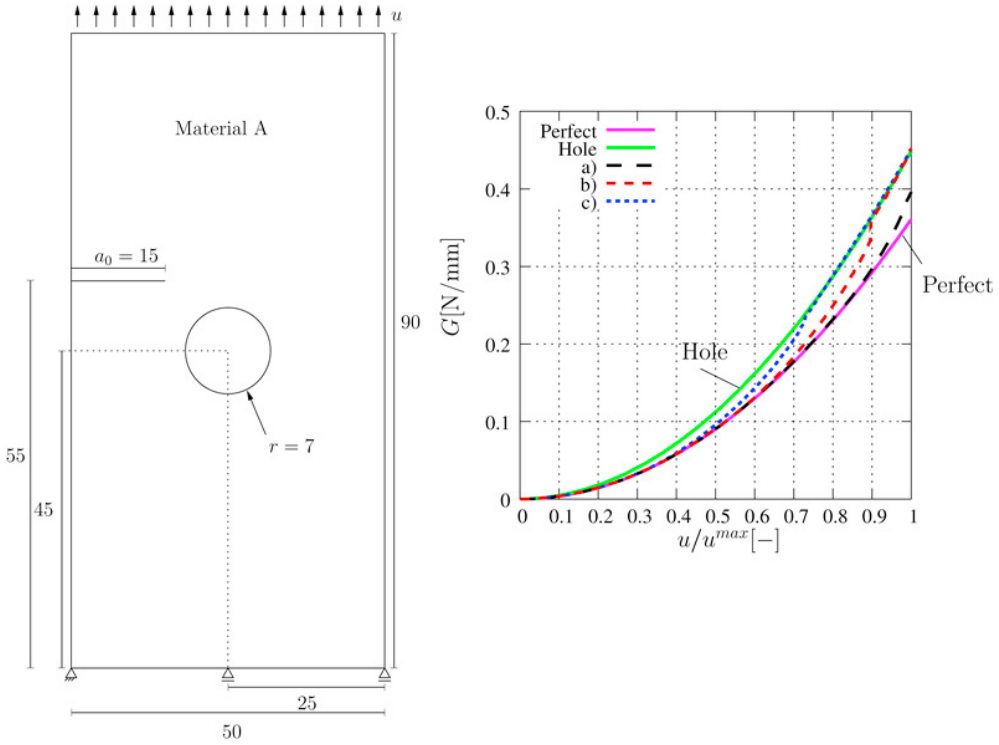

Fig. 5 Model for the crack tip loading analysis (size in mm, left), energy release rate versus the normalized displacement loading (right): a), b), c) from Tab. 1.

Acknowledgements

Financial support by the DFG is gratefully acknowledged.

References

Hashin, Z., 2002. Thin interphase/imperfect interface in elasticity with application to coated fiber composites. Journal of the Mechanics and Physics of Solids 50, 2509-2537.

Judt, P., Ricoeur, A., 2013a. Accurate loading analyses of curved cracks under mixed-mode conditions applying the J-integral. International Journal of Fracture 182, 53-66.

Judt, P., Ricoeur, A., 2013b. Quasi-static simulation of crack growth in elastic materials considering internal boundaries and interfaces. Key Engineering Materials 525-526, 181-184.

Judt, P., Ricoeur, A., Linek, G., 2015. Crack path prediction in rolled aluminum plates with fracture toughness orthotropy and experimental validation. Engineering Fracture Mechanics 138, 33-48.

Judt, P., Ricoeur, A., 2016. Numerical investigations in structures with imperfect material interfaces and cracks. Proceeding in Applied Mathematics and Mechanics 16, 143-144.

Kikuchi, M., Wada, Y. , Li, Y., 2016. Crack growth simulation in heterogeneous material by S-FEM. Engineering Fracture Mechanics 167, 239-247.

Ottosen,, N. S., Ristinmaa, M., Mosler, J., 2015. Fundamental physical principles and cohesive zone models at finite displacements- Limitations and possibilities. International Journal of Solids 53, 70-79.

Tilbrook, M. T., Rozenburg, K., Steffler, E. D., Rutgers, L., Hoffman, M., 2006. Crack propagation paths in layered, graded composites. Composites Part B: Engineering 37, 490-498.